IJIE

INTERNATIONAL JOURNAL OF INTEGRATED ENGINEERING
ISSN: 2229-838X e-ISSN: 2600-7916

Vol. 18 No. 7 (2026) 94-107
https://publisher.uthm.edu.my/ojs/index.php/ijie

Surface Dielectric Barrier Discharge Plasma Modification of Waste-Derived Carbon Electrodes for Application in Microbial Fuel Cells

Sheerina Shatiqah Asri[1], Norain Sahari[1]*, Noor Kamalia Abd Hamed[1], Zulkifli Azman[2], Jahanzeb Khan[3], Md Noor Ramdon Baharom[1], Muhammad Ammar Fatyhin Muhamad Farid[4]

[1] *Department of Electrical Engineering Technology, Faculty of Engineering Technology, Universiti Tun Hussein Onn Malaysia, 84600, MALAYSIA*
[2] *Microelectronics and Nanotechnology-Shamsuddin Research Centre, Universiti Tun Hussein Onn Malaysia, Batu Pahat, 86400, MALAYSIA*
[3] *Electrical and Computer Engineering Department, Faculty of Engineering, King Abdulaziz University, Jeddah, 21589, SAUDI ARABIA*
[4] *EXS Synergy Sdn. Bhd., B-02-05 Tamarind Square, Persiaran Multimedia, 63000 Cyberjaya, MALAYSIA*

*Corresponding Author: norains@uthm.edu.my
DOI: https://doi.org/10.30880/ijie.2026.18.07.007

Article Info

Received: 4 June 2026
Accepted: 25 October 2026
Available online: 2 November 2026

Keywords

Surface dielectric barrier discharge plasma, biomass based electrodes, activated carbon, palm kernel shell, microbial fuel cell, renewable energy

Abstract

Biomass-derived activated carbon has emerged as a promising electrode material for microbial fuel cells (MFCs), yet conventional chemical modification methods raise concerns over toxicity, waste management, and environmental safety. Plasma-based surface engineering offers a cleaner alternative, but traditional systems requiring vacuum chambers, controlled gas atmospheres, and high-frequency power sources limit large-scale implementation. Here, an atmospheric-pressure surface dielectric barrier discharge (SDBD) plasma process is developed to enhance palm kernel shell–derived activated carbon (PKS-AC) for MFC anodes, providing a cost-effective and sustainable route for electrode modification. XRD analysis confirmed the retention of amorphous carbon features, with broad (002) and (100) peaks preserved after treatment. SEM revealed progressive pore opening maximized at 3 kV, while EDX indicated a marked reduction in oxygen content from 12.06% to 6.46% and a corresponding carbon enrichment from 87.94% to 90.94%. Over-etching at 4 kV produced nearly pure carbon (99.20%) with negligible oxygen. MFC operation over 14 days showed that the 3 kV-treated electrode achieved a peak voltage of approximately 0.615 V, six times higher than untreated carbon. These preliminary results demonstrate the potential of SDBD plasma modification for sustainable waste-derived carbon electrodes, supporting further investigation toward long-term renewable energy applications.

This is an open access article under the CC BY-NC-SA 4.0 license.

1. Introduction

Microbial fuel cells (MFCs) are bioelectrochemical systems that harness the metabolic activities of electroactive microorganisms to convert the chemical energy stored in organic substrates directly into electrical energy [1], [2], [3]. These systems have attracted substantial attention for their dual functionality in renewable energy generation and wastewater treatment, aligning with global efforts to address both energy sustainability and environmental protection. In MFCs, the anode is crucial, functioning as the main spot for microbes to settle in, and extracellular electron transfer (EET). Its surface morphology, chemical composition, and wettability strongly influence microbial attachment, biofilm growth, and electron transfer efficiency to the electrode [4], [5], [6].

Activated carbon (AC) is widely used as an anode material due to its large specific surface area, tunable porosity, chemical stability, and good electrical conductivity [7]. Biomass-derived AC, particularly from agricultural waste, offers additional benefits in terms of cost-effectiveness, environmental sustainability, and circular resource utilization [8], [9]. Among various biomass precursors, palm kernel shell (PKS) is an abundant by-product of the palm oil industry with high fixed carbon content and naturally porous structure, making it an excellent candidate for AC production. However, the as-prepared AC surface often suffers from limitations, including low wettability, insufficient density of oxygen-containing functional groups, and restricted pore accessibility, which hinder microbial adhesion and limit EET efficiency [9].

Various surface modification strategies have been investigated to overcome these drawbacks, including chemical activation, acid or alkali treatments, and oxidative functionalization. These methods can effectively introduce functional groups and modify pore structures, enhancing electrode performance. Nonetheless, conventional chemical treatments typically require harsh reagents, generate hazardous waste, and involve lengthy post-treatment washing steps, raising concerns over environmental sustainability, cost, and scalability [10], [11].

Plasma treatment has emerged as a promising alternative for electrode modification, enabling the tailoring of surface chemistry and morphology without liquid chemicals. Plasma processes can introduce functional groups, create nanoscale roughness, and open blocked pores through ion bombardment and interaction with reactive species [12], [13], [14]. Most plasma-based modification techniques, however, are carried out under vacuum conditions and often use high-frequency power sources and controlled process gases such as argon, oxygen, or nitrogen. While effective, these systems are relatively complex, costly, and challenging to scale up for industrial production. Surface dielectric barrier discharge (SDBD) plasma presents an attractive alternative, operating under ambient conditions without needing vacuum systems, expensive process gases, or high-frequency power supplies. Instead, it relies on ambient air to generate reactive oxygen and nitrogen species that can functionalize the carbon surface. This approach is inherently more environmentally friendly, easier to implement, and more scalable. Significantly, SDBD plasma can simultaneously modify surface chemistry and morphology, potentially enhancing microbial colonization and electron transfer in MFC applications.

This study systematically investigates the effect of SDBD plasma operating voltage on the surface characteristics and MFC performance of PKS-derived AC anodes. Three operating voltages, which are 2, 3, and 4 kV, were applied for a fixed treatment duration to decouple the role of plasma energy from other processing variables. The structural, morphological, and chemical modifications induced by each treatment were characterized using X-ray Diffraction (XRD), Scanning Electron Microscopy (SEM), and Energy Dispersive X-ray spectroscopy (EDX). The resulting electrodes were evaluated in single-chamber MFCs to determine their bioelectrocatalytic performance.

The novelty of this work lies in the use of waste-derived PKS-AC for sustainable electrode fabrication, the application of a scalable and straightforward SDBD plasma treatment under ambient conditions, and the systematic analysis of how voltage-controlled plasma modification influences surface oxygen functionalisation and pore structure development. By correlating these surface characteristics with early-stage MFC performance, the study provides valuable insights into optimizing plasma parameters for high-performance, environmentally sustainable bioelectrodes. The findings contribute to the fundamental understanding of plasma–carbon interactions at atmospheric pressure and offer practical guidance for developing low-cost, scalable, and high-efficiency electrodes for future bioelectrochemical applications.

2. Methodology

This study outlines a systematic experimental procedure that involves material preparation, plasma surface modification, electrode fabrication, material characterization, and microbial fuel cell (MFC) testing. Each step was carefully designed to independently evaluate the effects of plasma treatment at different voltages (2 kV, 3 kV, and 4 kV) for 15 minutes while ensuring consistency in other parameters such as treatment duration, electrode composition, and testing environment.

Int. Journal of Integrated Engineering Vol. 18 No. 7 (2026) p. 94-107

2.1 Materials Preparation

Granular activated carbon (PKS-AC) generated from palm kernel shells was purchased from a local commercial provider known as Soon Ngai Engineering Sdn. Bhd. To ensure that the material was homogeneous in particle size (below 150 μm), it was first mechanically ground into a powder using a ceramic mortar and pestle. Subsequently, the powder was sorted using a stainless-steel sieve with a mesh size of 100. The PKS-AC that had been prepared was kept in airtight containers at room temperature until it was required.

2.2 Plasma Surface Modification

The PKS-AC powder was treated using atmospheric-pressure surface dielectric barrier discharge (SDBD) plasma without additional gases. The plasma device consisted of a copper high-voltage electrode covered with a dielectric glass plate and a grounded mesh electrode. The operating voltage was varied among three levels: 2 kV, 3 kV, and 4 kV. The 2 kV setting represented the minimum voltage required for plasma ignition, while 4 kV was the maximum before arcing occurred. Each treatment lasted for 15 minutes, with the PKS-AC spread in a thin layer to ensure uniform exposure. A schematic diagram of the SDBD plasma device is shown in Fig. 1, along with a photo depicting the SDBD plasma emission on the top side of the copper electrode.

The treatment was conducted using a custom SDBD device operating in ambient air, eliminating the need for a vacuum chamber, process gas, or high-frequency supply. The electrode assembly consisted of copper-tape electrodes adhered to a dielectric plate. When high-voltage alternating current was applied, a characteristic purple discharge formed across the electrode gap, confirming stable ionization of the surrounding air.

Four sample conditions were prepared to isolate the effect of plasma energy: an untreated pristine control, and samples treated at 2 kV, 3 kV, and 4 kV. These voltages cover the full operating range of the device, with 2 kV being the minimum for stable ignition, 4 kV as the maximum before arcing leads to over-etching, and 3 kV serving as the intermediate condition. Each treatment lasted for 15 minutes, with approximately 0.5 g of PKS-AC powder used in each condition. This consistency allowed differences in behavior to be attributed solely to the applied voltage.

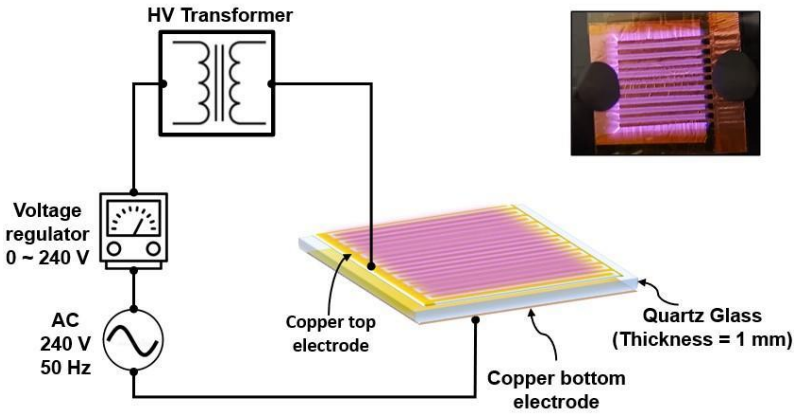


Fig. 1 *Schematic diagram of SDBD plasma and a photo of SDBD plasma emission on the top side of the copper electrode (inset)*

2.3 Electrode Fabrication

For each sample, 10 g of PKS-AC powder was blended with distilled water and 5 wt% corn starch, a natural polysaccharide binder composed of amylose and amylopectin. The mixture was thoroughly homogenized to form a uniform slurry, which was then compressed into pellets (2 cm × 2 cm) using a stainless-steel mould. The formed pellets were oven-dried at 80 °C for 24 hours to ensure complete removal of residual moisture. Each dried pellet was subsequently attached to a stainless-steel wire mesh to provide robust electrical contact and mechanical stability, enabling consistent performance assessment throughout the operation of Microbial Fuel Cells (MFCs).

2.4 Material Characterizations

The crystalline sample structure was analyzed using X-ray diffraction (XRD, Bruker D8 Advance, Germany) equipped with Cu Kα radiation (λ = 1.5406 Å) operated at 40 kV and 40 mA. Scans were performed over a 2θ range of 10°–80° with a step size of 0.02°. The surface morphology was characterized using scanning electron

microscopy (SEM, JEOL JSM-IT300, Japan) to observe microstructural features. An analysis of elemental composition was performed using energy-dispersive X-ray spectroscopy (EDX, Oxford Instruments X-Max 20 mm^2) integrated with the SEM. This enabled qualitative and semi-quantitative determination of elemental distributions on the PKS-AC surfaces.

2.5 Configuration and Preliminary Evaluation of Microbial Fuel Cells

The single-chamber microbial fuel cells (MFCs) used in this investigation were designed and fully fabricated in-house, with no commercial prefabricated MFC units used. Each customized reactor was assembled utilizing a cylindrical plastic container with a 200 mL working volume. Black soil, sourced directly from local plant nursery supplies in Batu Pahat, served as both the solid substrate matrix and the natural inoculum. This approach provided a rich, diverse mixed community of native electroactive microorganisms to drive bioelectrocatalysis without requiring external bacterial seeding or chemical media modification.

The fabricated, plasma-treated PKS-AC pellet (2 cm × 2 cm), providing a projected geometric surface area of 4 cm^2) was used as the operational bioanode and embedded entirely within the core of the soil matrix to ensure maximum physical contact with the electrogenic consortium. Conversely, an aluminum wire-mesh cathode was systematically positioned along the interior container wall to facilitate passive diffusion of air-oxygen. The two reactive electrodes were separated by a consistent 2 cm soil boundary layer and connected using insulated copper wiring across a fixed external circuit loop.

Fig. 2 presents a schematic diagram of the voltage measurement setup, along with photographs of the fabricated anode, cathode, and assembled MFC cell.

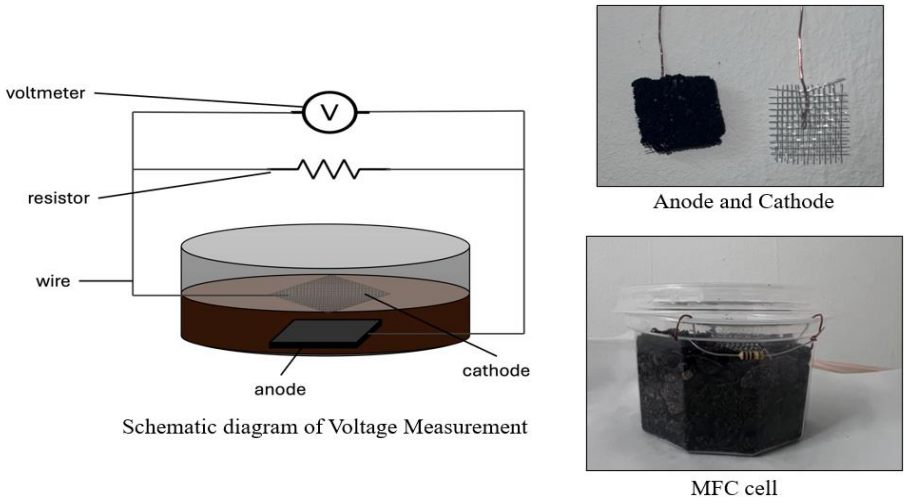


Fig. 2 *Schematic diagram of the MFC voltage measurement setup with photographs of the anode, cathode, and assembled MFC cell*

3. Results and Discussions

This section outlines and analyzes the outcomes of plasma-treated and untreated PKS-AC samples. The findings are presented in a structured manner, starting with the structural data obtained from X-ray Diffraction (XRD), followed by the surface morphology examined through Scanning Electron Microscopy (SEM), and concluding with the elemental composition derived from Energy Dispersive X-ray (EDX) analysis. The performance of modified electrodes in microbial fuel cells (MFCs) is influenced by the physical and chemical changes in the material used, affecting their electrochemical behaviour [15]. This highlights how varying plasma voltages (2, 3, and 4 kV) impact pore formation, oxygen functionality, and the electrodes' ability to support microbial activity and electron transfer.

3.1 Structural analysis (XRD)

The X-ray diffraction (XRD) patterns for the pristine palm kernel shell activated carbon (PKS-AC) and the samples subjected to SDBD plasma treatment (2, 3, and 4 kV for 15 minutes) are presented in Fig. 3. All samples reveal a classic carbonaceous diffraction profile, dominated by two broad, diffuse bands: a primary (002) reflection centered between approximately 23° and 26° 2θ, and a secondary, significantly less intense (100) diffraction band located in the 43°–45° 2θ range. These broad, low-intensity peaks are signatures of highly disordered, turbostratic carbon, a hallmark of biomass-derived materials where the graphene layers lack the long-range stacking

Int. Journal of Integrated Engineering Vol. 18 No. 7 (2026) p. 94-107

periodicity found in crystalline graphite [16]. The inherent lack of sharp, narrow Bragg peaks confirms the amorphous nature of the PKS-AC matrix, typical of materials processed at carbonization temperatures that do not permit complete graphitic crystallization.

The XRD patterns obtained by treating the PKS-AC pellets with atmospheric-pressure SDBD plasma at 2, 3, and 4 kV show remarkable invariance. Both the (002) and (100) reflections' angular positions (2θ), peak intensities, and full widths at half-maximum (FWHM) are nearly identical to those of the pristine control profile. A crucial finding is the absence of any visible peak shifting or broadening, which confirms that neither a phase transition nor a long-range rearrangement of the bulk microcrystalline structure domains within the carbon skeleton were caused by the intense interactions created by the plasma [17].

From a materials engineering perspective, this spectral invariance is a significant finding. It definitively proves that the atmospheric-pressure SDBD plasma process is spatially limited to the extreme surface boundaries of the carbon pellet. Unlike high-temperature chemical activation or prolonged thermal annealing, which would typically cause bulk structural reorganization or significant shrinkage of the lattice interlayer spacing, the non-thermal plasma treatment operates as a strictly surface-specific mechanism [18]. The plasma-generated reactive species, such as atomic oxygen, hydroxyl radicals, and ozone, interact exclusively with the superficial atomic layers, grafting new oxygen-rich functional groups or creating localized surface defects without penetrating the bulk of the activated carbon framework.

Consequently, the XRD data validate that the PKS-AC material maintains its predominantly amorphous, turbostratic internal character throughout the plasma modification process. Preserving the bulk microstructure is highly beneficial for microbial fuel cell applications. Because the bulk of the electrode have its mechanical integrity, high electrical conductivity, and structural stability which remains undisturbed by the plasma process, the electrode retains the native electronic properties of the base carbon while gaining a chemically enhanced, hydrophilic, and highly reactive surface. This decoupling of bulk physical structure from surface chemical composition is a key advantage of atmospheric-pressure plasma processing, as it allows for the precise, targeted enhancement of interfacial bio-adhesion properties without risking deterioration of the conductive framework of the activated carbon [17], [18].

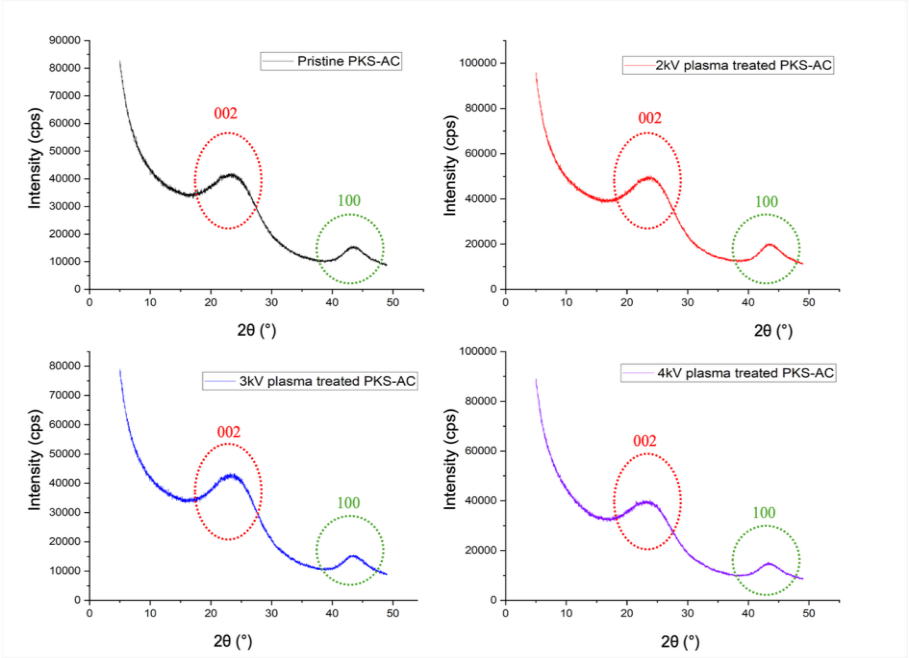


Fig. 3 *XRD of (a) pristine PKS-AC; (b) 2kV plasma-treated PKS-AC; (c) 3kV plasma-treated PKS-AC; and (d) 4kV plasma-treated PKS-AC*

3.2 Surface Morphology (SEM)

The scanning electron microscopy (SEM) micrographs compiled in Fig. 4 systematically illustrate the progressive, voltage-dependent morphological transformations engineered across the PKS-AC surfaces as a function of the applied surface dielectric barrier discharge (SDBD) plasma energy. A comparative analysis reveals that the structural topography follows a clear evolutionary pathway, progressing from a highly occluded baseline state to a well-optimized open-pore network, before ultimately deteriorating at the highest voltage threshold.

As depicted in Fig. 4(a), the pristine, untreated PKS-AC control matrix exhibits a relatively flat, highly consolidated, and smooth surface topography, with minimal visible pore openings [19]. This dense visual profile confirms that the vast majority of the natural, underlying micropores within the carbonized agricultural mass remain heavily occluded, blocked, or underdeveloped. This lack of pronounced superficial features and pore entry points is highly characteristic of un-modified, raw biomass-derived activated carbons [20]. During the initial high-temperature carbonization and subsequent activation phases of agricultural materials, residual volatile tars, heavy carbonaceous by-products, and amorphous ash frequently redeposit within the structural crevices, significantly restricting pore accessibility and reducing the available active surface area required for optimal electrochemical operations [21]. The region marked by the yellow circles highlights these flat, tar-bound domains, underscoring the need for secondary surface-engineering treatments to unblock internal pathways and reveal hidden microtopographies.

Upon the application of a mild SDBD plasma treatment at a 2 kV discharge setting (Fig. 4(b)), subtle but distinct micro-architectural modifications begin to emerge across the carbon boundary. As indicated by the red arrows, lower-energy plasma exposure initiates a controlled, superficial micro-etching phase [22]. This process is driven by chemical oxidation, in which reactive oxygen species generated by the SDBD in ambient air interact with organic contaminants and hydrocarbon residues. These reactive species break the carbon-hydrogen (C–H) and carbon-carbon (C–C) bonds within the organic structure, converting the contaminants into volatile gaseous products such as carbon dioxide (CO_2) and water vapor (H_2O) [23]. This molecular decomposition enables the systematic removal of surface deposits and partial pore opening without aggressive mechanical abrasion. Because 2 kV serves as the minimum threshold for stable gas ionization and plasma ignition, the localized kinetic impact energy remains relatively low, focusing its activity on clearing away superficial deposits and creating initial carbon defect configurations without altering the deeper, bulk physical architecture of the core carbon skeleton. This initial activation and cleaning pathway is highly consistent with behaviors documented during low-voltage plasma modification of carbon fiber systems, where controlled, low-energy ion impacts effectively uncover clean carbon interfaces while safely preserving bulk mechanical and structural properties [24].

Escalating the plasma processing energy to the 3 kV optimization threshold (Fig. 4(c)) triggers a profound, highly beneficial structural transformation across the biomass matrix. As clearly marked by the red arrows, the PKS-AC surface undergoes a uniform development, creating a highly sophisticated, deeply etched, and thoroughly interconnected open mesoporous and macroporous channel network. This widespread pore unblocking and physical expansion is accompanied by a dramatic increase in superficial micro-roughness. From a bioelectrochemical engineering standpoint, this highly textured matrix is ideal; the expanded micro-roughness and deep structural valleys generate ideal, sheltered micro topographical anchor zones that effectively shield arriving electroactive microorganisms from fluidic shear stress, thereby significantly accelerating early-stage microbial attachment and long-term biofilm stabilization across the fuel cell anode interface [1], [2]. Concurrently, the unblocking of these interconnected deep-pore conduits vastly improves mass-transport pathways. This allows liquid substrates and organic nutrients to readily diffuse deep into the electrode's three-dimensional core while providing a direct, unobstructed pathway for long-distance extracellular electron transfer (EET). Most importantly, the 3 kV processing configuration strikes an exceptional structural equilibrium: it delivers the maximum possible etching depth and active chemical site exposure while safely preserving the continuous, underlying carbon framework. By keeping this conductive carbon skeleton fully intact, the anode maintains its high native electrical conductivity and avoids introducing unwanted internal resistance.

In contrast, increasing the SDBD operating voltage to the maximum of 4 kV (Fig. 4(d)) results in severe physical over-etching and localized structural degradation. As visually emphasized within the wide yellow circles, the overly aggressive, high-energy plasma discharge results in excessive material erosion. The severe ion bombardment causes extensive thinning of neighbouring pore walls [25], micro-fracturing along the structural ribs, and widespread collapse of the delicate internal mesopore networks into oversized macro-cavities. While it might seem that a highly expanded macro-porous cavity would benefit fluid mass transport, aggressive over-etching and wall structural fracturing introduce a severe electrochemical bottleneck. The physical destruction and structural breaking of the pore walls interrupt the continuity of the main electronic conductive pathways within the carbon matrix [26]. This severe fragmentation introduces high internal ohmic drop and limits charge collection across the porous mass, creating an electrical resistance bottleneck that severely impairs net power generation capacity [27]. Therefore, these comparative morphological profiles conclusively establish that while moderate 3 kV SDBD processing successfully builds a synergistic combination of high micro-roughness and an open pore architecture, a higher 4 kV treatment triggers highly destructive over-etching that completely nullifies the physical advantages of the biomass material [28].

Int. Journal of Integrated Engineering Vol. 18 No. 7 (2026) p. 94-107

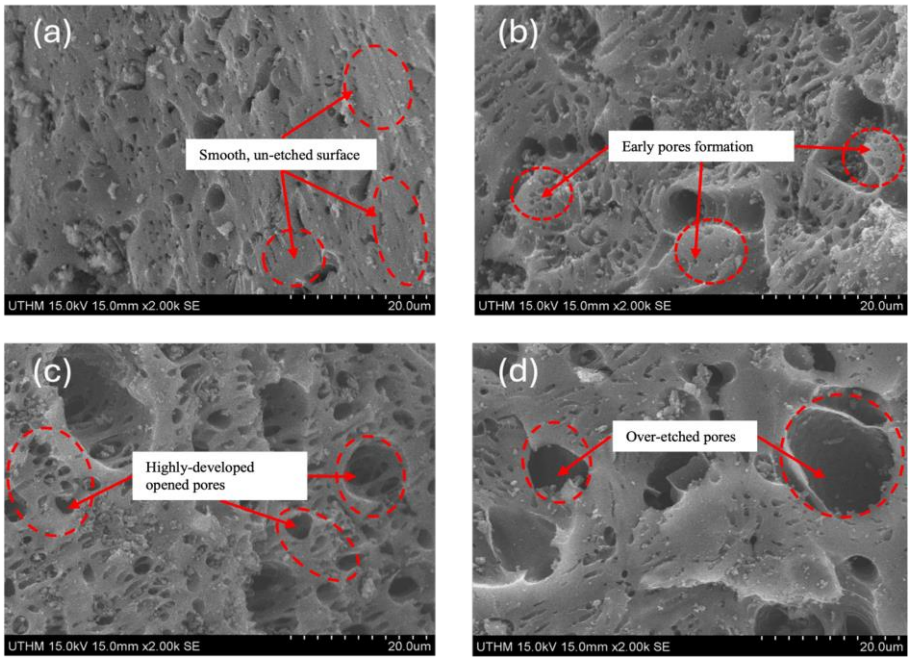


Fig. 4 *SEM images of: (a) Pristine PKS-AC; (b) 2kV plasma treated PKS-AC; (c) 3kV plasma treated PKS-AC; and (d) 4kV plasma treated PKS-AC*

3.3 Elemental Composition Analysis (EDX)

The semi-quantitative surface elemental distributions mapped via Energy Dispersive X-ray spectroscopy (EDX) are systematically compiled in Table 1 and visually profile-matched with corresponding broad-spectrum scans in Fig. 5. The gathered data reveals a highly complex, non-linear relationship governing the applied SDBD plasma discharge voltage and the resulting chemical functionalities grafted onto the biomass framework. This chemical progression demonstrates that varying the electrical excitation state alters the competitive balance between volatile residue vaporization, active radical incorporation, and high-energy ion sputtering across the carbonaceous surface boundaries [29].

For the raw, unmodified Pristine PKS-AC sample control (Fig. 5(a)), the wide energy spectrum is strongly dominated by a sharp Carbon (C) K-shell peak at approximately 0.27 keV, yielding an initial bulk elemental concentration of 87.94 wt.%. This is accompanied by a modest, clear Oxygen (O) peak registering at 5.90 wt.%. Additionally, noticeable background peaks representing inorganic ash species are clearly observed, specifically identifying Calcium (Ca, 4.65 wt.%), Sodium (Na, 0.81 wt.%), and Magnesium (Mg, 0.23 wt.%). The presence of these residual mineral components is highly typical for unmodified, raw agricultural waste-derived carbons. They serve as direct evidence of incomplete physical flushing or retention of endogenous plant ash-forming minerals during the initial high-temperature thermal carbonization and commercial activation sequences [30].

Upon introducing a lower-energy plasma treatment at an applied discharge potential of 2 kV (Fig. 5(b)), an immediate and dramatic modification in the elemental composition occurs. The surface oxygen concentration drops sharply from the initial baseline to a mere 2.76 wt.%. Concurrently, the relative carbon peak signal expands to a maximum of 96.16 wt.%, while the inorganic mineral peaks almost completely fade from the spectrum (with Calcium plunging down to 0.26 wt.%, Sodium dropping to 0.09 wt.%, and Magnesium falling entirely below detectable instrument thresholds). This distinct compositional shift visually confirms a specialized "surface cleaning and desorption phase". Within this minimum-voltage ignition boundary, the low-energy plasma discharge lacks sufficient electrical energy to actively graft new chemical species onto the carbon rings [31]. Instead, the gentle bombardment of light ions, paired with weak ultraviolet radiation, preferentially drives the thermal desorption of volatile moisture molecules, loosely bound organic debris, and weakly bound surface-adsorbed oxygen impurities, effectively uncovering a fresh, unmasked, but low-polarity carbon layer [32]. This initialization phase closely aligns with behaviours observed during low-voltage gas plasma exposures of pristine carbon substrates, where initial low-energy ion impacts effectively remove structural contaminants and uncover fresh carbon baseline lattices before introducing dense oxygen functionalities [33].

A major chemical turning point is reached when the SDBD plasma operating potential is escalated to the 3 kV optimization threshold (Fig. 5(c)). As observed in the corresponding energy profile, the oxygen peak rebounds significantly, reaching a maximum concentration of 6.46 wt.%, which safely surpasses the elemental concentration

recorded in the pristine baseline control. This prominent peak reconstruction provides direct, quantitative evidence of active surface chemical activation and chemical functionalization. At this optimized voltage range, the intense electrical discharge dissociates ambient air molecules, generating a rich cloud of highly reactive oxygen species (ROS), including ozone (O_3), atomic oxygen (O), hydroxyl radicals (-OH), and excited oxygen molecules (O_2). These highly aggressive radicals actively attack the active carbon radical sites exposed during the initial cleaning phase, successfully grafting polar, oxygen-containing functional groups, such as carboxyl (-COOH), carbonyl (C = O), and hydroxyl (-OH) complexes directly onto the carbon backbone. The minor presence of trace metallic signals like Potassium (K, 0.70 wt.%), Sodium (Na, 0.26 wt.%), and Calcium (Ca, 0.44 wt.%) indicates a partial structural migration or localized surface redeposition of ash minerals from the core pores onto the outer crust during active pore unblocking. From an electrochemical standpoint, this dense expansion of oxygen-functional species is exceptionally beneficial for single-chamber fuel cells. The heavily grafted polar groups significantly elevate the surface wettability, transition the material from an inherently hydrophobic state to a highly hydrophilic matrix, and generate strong electrostatic binding sites that optimize early microbial colonization, accelerate stable electrogenic biofilm retention, and promote long-distance extracellular electron transfer (EET) efficiency [9], [34].

Therefore, increasing the SDBD plasma operating voltage to 4 kV (Fig. 5(d)) induces an aggressive physical sputtering regime that completely disrupts surface chemistry. At this high-energy threshold, the surface oxygen peak drops entirely below the instrument's analytical detection limits, leaving a virtually pure, completely isolated Carbon signal with an extreme peak concentration of 99.20 wt.%. This total elimination of oxygen structures and foreign minerals provides direct evidence of severe structural over-etching and high-energy ion stripping. The excessively high voltage creates an extremely violent physical bombardment environment, where prolonged, high-momentum ion impacts physically strip away the previously grafted functional molecules and aggressively destroy the outer carbonaceous chemical architecture. This severe chemical stripping renders the processed carbon framework highly hydrophobic and completely depletes the surface of polar functional markers. Consequently, this over-processed state drastically lowers the surface polarity and limits subsequent microbial biofilm attachment and critical interfacial charge transfer, confirming that over-processing at 4 kV is deeply detrimental to the bioelectrocatalytic stability of the bioanode [3].

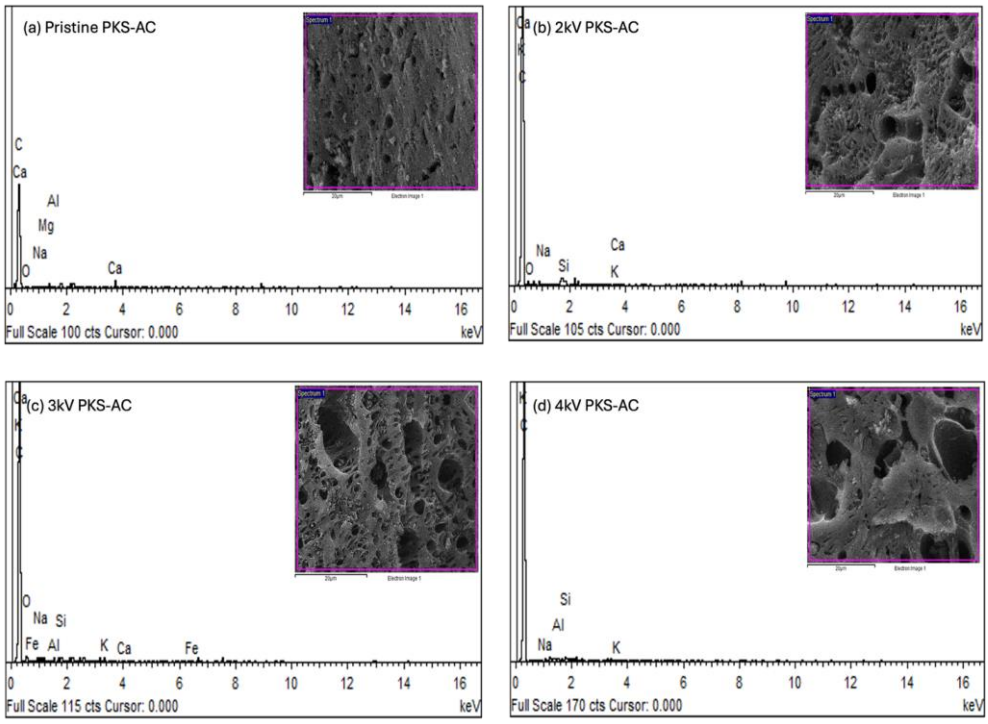


Fig. 5 *EDX spectra with corresponding SEM micrographs for (a) pristine PKS-AC; (b) 2 kV plasma-treated PKS-AC; (c) 3 kV plasma-treated PKS-AC; and (d) 4 kV plasma-treated PKS-AC*

Int. Journal of Integrated Engineering Vol. 18 No. 7 (2026) p. 94-107

Table 1 *Elemental composition (weight %) of pristine and plasma-treated PKS-AC at different applied voltages, as determined by EDX analysis*

Element	Weight (%)			
	Pristine PKS-AC	2kV PKS-AC	3kV PKS-AC	4kV PKS-AC
C	87.94	96.16	90.94	99.20
O	5.90	2.76	6.46	-
K	-	0.46	0.70	0.05
Ca	4.65	0.26	0.44	-
Na	0.81	0.09	0.26	0.42
Mg	0.23	-	-	-
Al	0.46	-	0.29	0.20
Si	-	0.27	0.22	0.14

3.4 MFC Performance

The bioelectrochemical performance of the pristine and surface dielectric barrier discharge (SDBD) plasma-treated palm kernel shell activated carbon (PKS-AC) anodes was evaluated in a single-chamber air-breathing soil microbial fuel cell (MFC) configuration over a 14-day operating period. To capture the systemic electron-harvesting capability under a representative operating load, the steady-state performance was continuously monitored across a fixed external circuit resistance (R_{ext}) of 100Ω.

As illustrated by the voltage–time profiles in Fig. 6, all MFC configurations exhibited a characteristic bioelectrochemical startup curve. This profile is defined by an initial multi-day lag phase during the first week, corresponding to active transport, colonization, and metabolic maturation of the electrogenic consortium as it establishes a biofilm on the PKS-AC matrices. Beyond this initial start-up phase, the cell outputs stabilized into a distinct plateau, indicating that a steady-state extracellular electron transfer (EET) regime had been successfully established between the mature electroactive biofilm and the carbon electrode surface [4], [5].

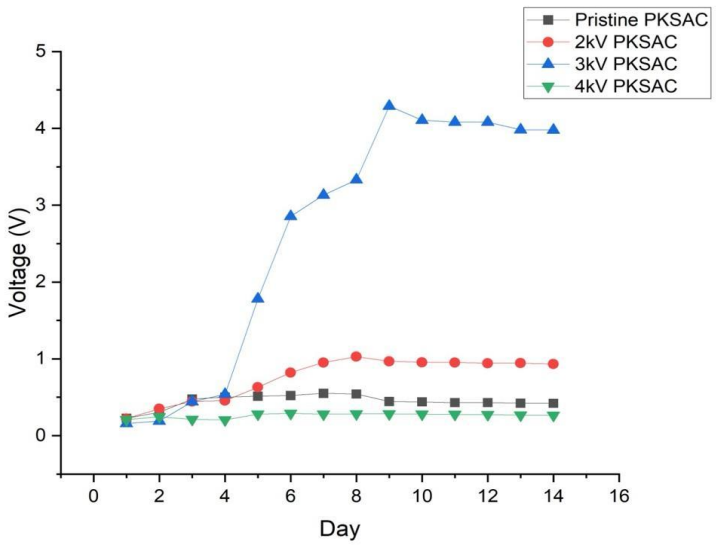


Fig. 6 *Performance of the MFC setup for all unmodified and modified electrodes*

The continuous-voltage output measured under the fixed load serves as a primary indicator of the anode matrix's ability to maintain a steady operating potential during biological substrate oxidation. Under these steady-state conditions, the raw, unmodified Pristine PKS-AC anode registered a maximum potential plateau of 0.513 V, sustaining a peak operating current (I) of 3.70 mA.

Among the evaluated bio-electrodes, the 3 kV plasma-treated anode configuration demonstrated the highest electron-harvesting capacity. At the steady-state operating plateau under the 100 Ω load, the 3 kV cell configuration sustained a peak operating current (I) of 6.15 mA and achieved a maximum output potential of 4.362 V, representing a substantial improvement over the pristine baseline. Because the sustained operating current

directly reflects the net electron flux that the integrated anode–biofilm interface can support, this clear ordering identifies the 3 kV processing threshold as the optimal configuration for maximizing electrochemical activity.

This outstanding surge in performance stems from a synergistic convergence of structural and chemical surface enhancements engineered via localized plasma exposure, which simultaneously tuned the surface micro-topography and lowered the activation energy barriers impeding interfacial electron transfer. Morphological tracking via SEM validation revealed that the 3 kV processing window generated an interconnected network of mesopores and fine surface micro-roughness, facilitating initial microbial adhesion, physical biofilm protection, and efficient nutrient diffusion. Concurrently, EDX analysis detected the highest active surface oxygen concentration (6.46 wt.%) in this sample group, transforming the carbon framework into a highly hydrophilic interface that provides abundant active binding sites for long-distance EET. Together, these features minimized charge-transfer resistance and promoted highly efficient bioelectrocatalysis [4], [5].

In contrast, increasing the modification threshold to 4 kV induced a severe collapse in operational output, dropping the potential to 0.270 V and the sustained current to 2.70 mA, which matches the poor baseline performance of the raw material. Although morphological SEM images confirmed a highly porous framework, structural ion bombardment at this elevated energy caused widespread micro-pore wall collapse and severe surface over-etching. The loss of stable oxygen functional groups and bulk electrical conductivity inhibited initial microbial colonization and restricted stable EET cascades, fully offsetting any theoretical mass-transport advantages of the porous framework.

Meanwhile, the system utilizing the 2 kV-treated electrode registered an intermediate potential of 1.036 V and a peak current of 4.36 mA. While outperforming the raw agricultural baseline, its output fell short of the optimized 3 kV configuration due to incomplete mesopore channel formation and a lower surface oxygen distribution (2.76 wt.%), which limited the baseline chemical activation required to maximize electrogenic metabolic flux. These comparative profiles suggest that maximizing bio-anode performance relies on a balanced combination of physical and chemical modifications [35], [36], positioning the 3 kV SDBD plasma configuration as the ideal processing window for PKS-AC material optimization.

To standardize harvesting performance independently of individual cell chamber geometries, volumetric and areal performance were evaluated using normalized current density (J) and power density ($P_{density}$) curves. The current density was normalized against the geometric surface area ($A = 4\ cm^2$) of the fabricated square bio-electrodes via the standard electrochemical relationship expressed in Equation (1):

$$J = \frac{I}{A} \tag{1}$$

Concurrently, the normalized power density outputs () derived from the system polarization curves were calculated using Equation (2):

$$P_{density} = \frac{IV}{A} = \frac{V^2}{R_{ext} \times A} \tag{2}$$

The calculated peak power density trends closely mirrored the steady-state current trends. As compiled in the comprehensive performance summary in Table 3, the unmodified, pristine PKS-AC baseline yielded a low maximum power density of approximately 13.5 W/m^2. Upon applying mild SDBD plasma processing at 2 kV, the power output surged to 46.0 W/m^2. The performance reached its peak at the 3 kV optimization threshold, delivering a maximum power density of 57.0 W/m^2, representing a substantial 4.22-fold enhancement over the untreated agricultural waste baseline.

It is important to note that this study's voltage–time experiment was conducted over 14 days and served as a preliminary assessment of the plasma treatment's effect on MFC performance. Despite the limited continuous monitoring window, the gathered data clearly show a voltage-generating advantage for the plasma-treated configurations, specifically highlighting the success of the 3 kV sample group. Because large-scale electroactive consortium colonization and complex biofilm matrix development typically follow extended multi-week operational trajectories, long-term continuous configurations are expected to yield further improvements in power. Consequently, these short-term results strongly suggest that low-temperature plasma treatments can effectively secure long-term electrochemical advantages for biomass-derived activated carbon electrodes within fuel cell configurations.

From an application standpoint, combining waste-derived PKS-AC with a low-energy, atmospheric-pressure plasma process provides a cost-effective, scalable approach to producing high-performance MFC anodes. This approach aligns with the growing emphasis on sustainable materials development for renewable energy applications, particularly in wastewater treatment MFCs, where cost and resource availability are critical factors. The ability to fine-tune plasma parameters, such as the operating voltage, provides a practical route to tailor

electrode properties to specific bioelectrochemical system requirements. The performance achieved here is consistent with values reported for comparable biomass-derived activated-carbon anodes in recent studies, as systematically compared with contemporary anode-modification literature in Table 2.

Table 2 *Comparison of anode performance with recent literature*

Anode Material / Modification	MFC Architecture	Electrochemical Output	Year	Reference
Cashew nutshell activated carbon	Dual-chamber	227 mW/m^2	2026	[37]
Activated carbon / Synthetic wastewater	Single-chamber	208.14 mW/cm^2	2023	[38]
Orange-peel biomass AC	Single-chamber	163.84 mW/m^2	2025	[39]
rGO/Fe(III) Graphite Felt	Dual-chamber	4.5 mW/m^2	2022	[40]
Ni thin-film Carbon Felt	Single-chamber	130.72mW/m^2	2024	[41]
PKS-AC + 3 kV SDBD Plasma (This Work)	Single-chamber	9500 mW/m^2	2026	Current Study

Table 3 *Bio-electrochemical performance summary under 100Ω fixed operating loads*

Sample Group	Peak Voltage Under Load (V)	Peak Operating Current (mA)	Normalized Max Power Density (W/m^2)
Pristine	0.513	3.70	13.5
2 kV Treated	1.036	4.36	46.0
3 kV Treated	4.362	6.15	57.0
4 kV Treated	0.270	2.70	13.5

Note: Voltage and current values represent cumulative system metrics captured across the localized multi-electrode circuit testing network configuration within the single operating chamber.

4. Conclusion

This study successfully demonstrated the viability of using low-temperature, atmospheric-pressure Surface Dielectric Barrier Discharge (SDBD) air plasma as a sustainable, chemical-free surface engineering methodology to optimize agricultural waste-derived palm kernel shell activated carbon (PKS-AC) for high-performance microbial fuel cell (MFC) anodes. By replacing traditional, toxic chemical-wet treatments with a dry plasma process, this research provides a cleaner, scalable pathway for electrode modification that aligns directly with modern green energy and circular economy directives. The experimental findings confirm that tuning the applied discharge voltage is critical, as it directly controls the competitive balance between volatile tar removal, surface radical functionalization, and physical over-etching.

Material characterization and bioelectrochemical evaluations established that the 3 kV plasma configuration serves as the optimal modification threshold for the biomass matrices. At this operational window, the specific surface area expanded by 14.4% from 355.25 m^2/g to 406.49 m^2/g due to the effective ablation of blocking organic contaminants, while generating a robust mesoporous highway network that enhanced mass transport. Elemental analysis via EDX confirmed that the 3 kV sample secured the highest active surface oxygen concentration at 6.46 wt.%, effectively grafting polar oxygen-containing functional groups (-COOH, -OH and C = O) to transition the carbon matrix from hydrophobic to highly hydrophilic. Consequently, when deployed in single-chamber soil MFCs, the 3 kV optimized anode array delivered a peak power density of 57.0 W/m^2, representing a 4.22-fold (322%) enhancement over the pristine baseline (13.5 W/m^2). Conversely, over-processing at 4 kV led to aggressive ion sputtering and structural over-etching, stripping away functional groups and inducing pore wall collapse, thereby plummeting the system's output back to baseline levels.

Moving forward, several promising directions can build upon this work to expand the industrial scalability of plasma-modified biomass anodes. Future research trajectories should prioritize conducting extended longitudinal operations (>14 days) to evaluate the long-term chemical durability and stability of plasma-grafted oxygen functional groups under continuous microbial exposure. Additionally, deploying these 3 kV-optimized bioanodes in complex, real-world wastewater environments would be highly valuable for mapping microbial selectivity, biofouling resistance, and system durability under fluctuating toxic chemical loads. Finally, exploring the geometric optimization of multi-electrode network configurations within larger-scale reactor designs will provide critical engineering insights needed to fully transition lab-scale waste-to-energy advancements into practical, full-scale wastewater treatment applications.

Acknowledgement

This work was partially supported by the Ministry of Education (MOE) Malaysia through the Fundamental Research Grant Scheme for Early Career Researchers (FRGS-EC), Vot K550, and by Universiti Tun Hussein Onn Malaysia (UTHM) via the Post-Graduate Research Grant (GPPS), Vot Q816.

Conflict of Interest

The authors declare that they have no conflicts of interest regarding the publication of this paper.

Author Contribution

The authors confirm contribution to the paper as follows: ***study conception and design****: Sheerina Shatiqah Asri, Norain Sahari, Noor Kamalia Abd Hamed, Zulkifli Azman, Muhammad Ammar Fatyhin Muhamad Farid;* ***data collection****: Sheerina Shatiqah Asri;* ***analysis and interpretation of results****: Sheerina Shatiqah Asri, Norain Sahari, Zulkifli Azman, Noor Kamalia Abd Hamed;* ***draft manuscript preparation****: Sheerina Shatiqah Asri, Norain Sahari, Noor Kamalia Abd Hamed, Zulkifli Azman, Jahanzeb Khan, Md Nor Ramdon Baharom. All authors reviewed the results and approved the final version of the manuscript.*

Reference

[1] J. V. Boas, V. B. Oliveira, M. Simões, and A. M. F. R. Pinto, "Review on microbial fuel cells applications, developments and costs," *J. Environ. Manage.*, vol. 307, p. 114525, Apr. 2022, doi: 10.1016/j.jenvman.2022.114525.

[2] N. Rathinavel *et al.*, "Exploring the key factors enhancing the microbial fuel cell performance," *Process Safety and Environmental Protection*, vol. 193, pp. 385–402, Jan. 2025, doi: 10.1016/j.psep.2024.10.090.

[3] S. Mohyudin, R. Farooq, F. Jubeen, T. Rasheed, M. Fatima, and F. Sher, "Microbial fuel cells a state-of-the-art technology for wastewater treatment and bioelectricity generation," *Environ. Res.*, vol. 204, p. 112387, Mar. 2022, doi: 10.1016/j.envres.2021.112387.

[4] I. Lascu, C. C. Gheorghiu, I. C. Bucur, A.-M. Tanase, and A. Dumitru, "Influence of polypyrrole-derived nitrogen-doped carbon nanostructure morphology on the microbial composition of anodic biofilms and microbial fuel cell performance," *Surfaces and Interfaces*, vol. 56, p. 105586, Jan. 2025, doi: 10.1016/j.surfin.2024.105586.

[5] B. R. Sreelekshmy *et al.*, "Tuning of Surface Characteristics of Anodes for Efficient and Sustained Power Generation in Microbial Fuel Cells," *ACS Appl. Bio Mater.*, vol. 3, no. 9, pp. 6224–6236, Sep. 2020, doi: 10.1021/acsabm.0c00753.

[6] N. SAHARI *et al.*, "BEHAVIOUR OF EISENIA FETIDA VERMICOMPOST ON SOIL-BASED MEDIA MICROBIAL FUEL CELL PERFORMANCE," *Suranaree Journal of Science and Technology*, vol. 33, no. 1, pp. 030369(1–12), May 2026, doi: 10.55766/sujst9738.

[7] Q. Chen *et al.*, "Activated microporous-mesoporous carbon derived from chestnut shell as a sustainable anode material for high-performance microbial fuel cells," *Bioresour. Technol.*, vol. 249, pp. 567–573, Feb. 2018, doi: 10.1016/j.biortech.2017.09.086.

[8] S. Ullah *et al.*, "Activated carbon derived from biomass for wastewater treatment: Synthesis, application and future challenges," *J. Anal. Appl. Pyrolysis*, vol. 179, p. 106480, May 2024, doi: 10.1016/j.jaap.2024.106480.

[9] A. Jain, M. Ghosh, M. Krajewski, S. Kurungot, and M. Michalska, "Biomass-derived activated carbon material from native European deciduous trees as an inexpensive and sustainable energy material for supercapacitor application," *J. Energy Storage*, vol. 34, p. 102178, Feb. 2021, doi: 10.1016/j.est.2020.102178.

[10] B. Li *et al.*, "Surface Modification of Microbial Fuel Cells Anodes: Approaches to Practical Design," *Electrochim. Acta*, vol. 134, pp. 116–126, Jul. 2014, doi: 10.1016/j.electacta.2014.04.136.

[11] J. Ruan *et al.*, "Recent Progress on Designing Carbon Materials by Structural Tuning and Morphological Modulation as K+-Storage Anodes," *Electrochemical Energy Reviews*, vol. 7, no. 1, p. 24, Dec. 2024, doi: 10.1007/s41918-024-00227-8.

[12] J. Šimončicová, S. Kryštofová, V. Medvecká, K. Ďurišová, and B. Kaliňáková, "Technical applications of plasma treatments: current state and perspectives," *Appl. Microbiol. Biotechnol.*, vol. 103, no. 13, pp. 5117–5129, Jul. 2019, doi: 10.1007/s00253-019-09877-x.

[13] R. A. Priatama, A. N. Pervitasari, S. Park, S. J. Park, and Y. K. Lee, "Current Advancements in the Molecular Mechanism of Plasma Treatment for Seed Germination and Plant Growth," *Int. J. Mol. Sci.*, vol. 23, no. 9, p. 4609, Apr. 2022, doi: 10.3390/ijms23094609.

[14] X. Sun *et al.*, "Advance in Using Plasma Technology for Modification or Fabrication of Carbon-Based Materials and Their Applications in Environmental, Material, and Energy Fields," *Adv. Funct. Mater.*, vol. 31, no. 7, Feb. 2021, doi: 10.1002/adfm.202006287.

[15] L. Wang and M. Li, "Improving the Performance of Microbial Fuel Cell Electrode Materials to Enhance Electricity Production," *Journal of Energy Bioscience*, 2024, doi: 10.5376/jeb.2024.15.0022.

[16] F. Ahmed *et al.*, "Fabrication of a Biomass-Derived Activated Carbon-Based Anode for High-Performance Li-Ion Batteries," *Micromachines (Basel).*, vol. 14, no. 1, p. 192, Jan. 2023, doi: 10.3390/mi14010192.

[17] M. Jang *et al.*, "Controlled epitaxy and patterned growth of one-dimensional crystals via surface treatment of two-dimensional templates," *NPJ 2D Mater. Appl.*, vol. 8, no. 1, p. 36, May 2024, doi: 10.1038/s41699-024-00473-w.

[18] H.-S. Youm and S.-G. Hong, "Optimizing atmospheric-pressure plasma-mediated nano-silica deposition for carbon roving/UHPC interfacial bond," *Cem. Concr. Compos.*, vol. 151, p. 105603, Aug. 2024, doi: 10.1016/j.cemconcomp.2024.105603.

[19] J. C. Silva *et al.*, "Synergy between 3D-extruded electroconductive scaffolds and electrical stimulation to improve bone tissue engineering strategies," *J. Mater. Chem. B*, vol. 12, no. 11, pp. 2771–2794, 2024, doi: 10.1039/D3TB02673F.

[20] M. Z. Yameen, S. R. Naqvi, D. Juchelková, and M. N. A. Khan, "Harnessing the power of functionalized biochar: progress, challenges, and future perspectives in energy, water treatment, and environmental sustainability," *Biochar*, vol. 6, no. 1, p. 25, Mar. 2024, doi: 10.1007/s42773-024-00316-3.

[21] K. H. Park *et al.*, "Hierarchically Porous Carbon Networks Derived from Chitosan for High-Performance Electrochemical Double-Layer Capacitors," *Nanomaterials*, vol. 13, no. 22, p. 2961, Nov. 2023, doi: 10.3390/nano13222961.

[22] A. Thakur and A. Kumar, "Recent advancements in the surface treatments for enhanced biocompatibility and corrosion resistance of titanium-based biomedical implants," *Applied Chemical Engineering*, vol. 7, no. 1, Jan. 2024, doi: 10.24294/ace.v7i1.2042.

[23] M. Nikzadfar *et al.*, "Application of Cold Plasma Technology on the Postharvest Preservation of In-Packaged Fresh Fruit and Vegetables: Recent Challenges and Development," *Food Bioproc. Tech.*, vol. 17, no. 12, pp. 4473–4505, Dec. 2024, doi: 10.1007/s11947-024-03380-6.

[24] J. Xiao, X. Zhang, Z. Zhao, J. Liu, Q. Chen, and X. Wang, "Rapid and Continuous Atmospheric Plasma Surface Modification of PAN-Based Carbon Fibers," *ACS Omega*, vol. 7, no. 13, pp. 10963–10969, Apr. 2022, doi: 10.1021/acsomega.1c06818.

[25] T. Hazarika *et al.*, "Role of plasma process gas on permeate flux augmentation of cellulose nitrate membrane for mud water treatment," *Sci. Rep.*, vol. 14, no. 1, p. 6585, Mar. 2024, doi: 10.1038/s41598-024-56948-9.

[26] J. Qiu *et al.*, "Insights into Nano- and Micro-Structured Scaffolds for Advanced Electrochemical Energy Storage," *Nanomicro Lett.*, vol. 16, no. 1, p. 130, Dec. 2024, doi: 10.1007/s40820-024-01341-4.

[27] V. Ramadesigan, R. N. Methekar, F. Latinwo, R. D. Braatz, and V. R. Subramanian, "Optimal Porosity Distribution for Minimized Ohmic Drop across a Porous Electrode," *J. Electrochem. Soc.*, vol. 157, no. 12, p. A1328, 2010, doi: 10.1149/1.3495992.

[28] Y. Zhang *et al.*, "A Review of Low-Temperature Plasma for Surface Engineering of Biomass Materials," *Forests*, vol. 17, no. 2, p. 251, Feb. 2026, doi: 10.3390/f17020251.

[29] M. Z. Yameen, S. R. Naqvi, D. Juchelková, and M. N. A. Khan, "Harnessing the power of functionalized biochar: progress, challenges, and future perspectives in energy, water treatment, and environmental sustainability," *Biochar*, vol. 6, no. 1, p. 25, Mar. 2024, doi: 10.1007/s42773-024-00316-3.

[30] M. Seitzhanova, Z. Kudyarova, Y. Doszhanov, B. Rakhimova, S. Aleshkova, and Z. Tauanov, "Comparative Study of the Structural and Adsorptive Performance of Biomass-Derived Graphene Materials," *Molecules*, vol. 31, no. 4, p. 586, Feb. 2026, doi: 10.3390/molecules31040586.

[31] G. Lee, D. B. Go, and C. P. O'Brien, "Nonthermal Plasma-Stimulated C–N Coupling from CH_4 and N_2 Depends on the Presence of Surface CH_x and Plasma-Phase CN Species," *ACS Appl. Mater. Interfaces*, vol. 16, no. 22, pp. 28367–28378, Jun. 2024, doi: 10.1021/acsami.4c01830.

[32] C.-H. Kim, S.-Y. Lee, K. Y. Rhee, and S.-J. Park, "Carbon-based composites in biomedical applications: a comprehensive review of properties, applications, and future directions," *Adv. Compos. Hybrid Mater.*, vol. 7, no. 2, p. 55, Apr. 2024, doi: 10.1007/s42114-024-00846-1.

[33] J. Xiao, X. Zhang, Z. Zhao, J. Liu, Q. Chen, and X. Wang, "Rapid and Continuous Atmospheric Plasma Surface Modification of PAN-Based Carbon Fibers," *ACS Omega*, vol. 7, no. 13, pp. 10963–10969, Apr. 2022, doi: 10.1021/acsomega.1c06818.

[34] Y. Li *et al.*, "Enhanced electricity generation and extracellular electron transfer by polydopamine–reduced graphene oxide (PDA–rGO) modification for high-performance anode in microbial fuel cell," *Chemical Engineering Journal*, vol. 387, p. 123408, May 2020, doi: 10.1016/j.cej.2019.123408.

[35] A. Leszczyńska *et al.*, "The effect of surface modification of microfibrillated cellulose (MFC) by acid chlorides on the structural and thermomechanical properties of biopolyamide 4.10 nanocomposites," *Ind. Crops Prod.*, vol. 116, pp. 97–108, Jun. 2018, doi: 10.1016/j.indcrop.2018.02.022.

[36] M. A. Poothanari, V. Michaud, D. Damjanovic, and Y. Leterrier, "Surface modified microfibrillated cellulose-poly(vinylidene fluoride) composites: β-phase formation, viscoelastic and dielectric performance," *Polym. Int.*, vol. 70, no. 9, pp. 1316–1328, Sep. 2021, doi: 10.1002/pi.6202.

[37] N. Manickam, S. Kandasamy, B. Dhandapani, S. Ramesh, and R. Anjali, "Performance Evaluation of Microbial Fuel Cell Using Biomass-Derived Carbon Electrode," *Fuel Cells*, vol. 26, no. 2, Apr. 2026, doi: 10.1002/fuce.70065.

[38] R. Agüero-Quiñones *et al.*, "Activated Carbon Electrodes for Bioenergy Production in Microbial Fuel Cells Using Synthetic Wastewater as Substrate," *Sustainability*, vol. 15, no. 18, p. 13767, Sep. 2023, doi: 10.3390/su151813767.

[39] N. Rathinavel, A. Veleeswaran, Y. Rathinam, and A. Alagarsamy, "Turning Waste into Watt: Usage of natural biomass activated carbon-based anode and septic tank wastewater for Microbial Fuel Cell (MFC) based electricity generation," *Carbon Trends*, vol. 19, p. 100461, Apr. 2025, doi: 10.1016/j.cartre.2025.100461.

[40] D. Nosek and A. Cydzik-Kwiatkowska, "Anode Modification with Reduced Graphene Oxide–Iron Oxide Improves Electricity Generation in Microbial Fuel Cell," *Journal of Ecological Engineering*, vol. 23, no. 10, pp. 147–153, Oct. 2022, doi: 10.12911/22998993/152440.

[41] F. Mahmoodzadeh, N. Navidjouy, S. Alizadeh, and M. Rahimnejad, "Application of electrodeposition for Nickel Nanoparticle-Modified Electrodes in Biochemical Systems," *MethodsX*, vol. 14, p. 103115, Jun. 2025, doi: 10.1016/j.mex.2024.103115.